

Pyridine-Based Sulfoxide Pincer Complexes of Rhodium and Iridium

Thomas Schaub,[†] Udo Radius,[‡] Yael Diskin-Posner,[§] Gregory Leitus,[§]
Linda J. W. Shimon,[§] and David Milstein^{*·†}

Department of Organic Chemistry and Unit of Chemical Research Support, The Weizmann Institute of Science, Rehovot 76100, Israel, and Institute for Inorganic Chemistry, University of Karlsruhe, 76131 Karlsruhe, Germany

Received December 21, 2007

The new pyridine-based sulfoxide pincer ligand **1** (2-(diethylaminomethyl)-6-(*tert*-butylsulfinylmethyl)pyridine = S(O)NN) reacts cleanly with Rh₂(COE)₄Cl₂ to form the neutral water- and air-stable Rh^I complex [Rh(S(O)NN)(NCCH₃)], **1**. The cationic complexes [Rh(S(O)NN)(NCCH₃)]⁺[BF₄⁻] (**2**) and [Ir(S(O)NN)(COE)]⁺[BF₄⁻] (**5**) were obtained by the reaction of **1** with the appropriate metal precursors. The corresponding carbonyl complexes [Rh(S(O)NN)(CO)]⁺[PF₆⁻] (**4**) and [Ir(S(O)NN)(CO)]⁺[BF₄⁻] (**7**) exhibit νCO in the IR spectra that shows that ligand **1** is a relatively poor σ-donor ligand compared to the more common PNP-type ligands, resulting in rather electron-poor metal centers. The carbonyl compounds can be deprotonated to the remarkably stable dearomatized complexes Rh(S(O)NN*)(CO) (**8**) and Ir(S(O)NN*)(CO) (**9**). DFT studies on **8** revealed a high electron delocalization over the pyridine ring system and the sulfur atom, which explains the high stability of **8** toward reprotonation. Complete protonation of **8** was achieved in acetic acid.

Introduction

Pincer complexes of the late transition metals have attracted much attention over the last two decades because of their ability

to activate different strong bonds as well as their high activity in many catalytic transformations.¹ In the last years, our research was mainly focused on the chemistry of electron-rich tridentate PCP,² PCN,³ PCO,⁴ PNP,⁵ and PNN⁶ systems. A disadvantage of these very versatile ligands lies in their air-sensitive and toxic phosphine groups, prompting us to search for alternatives that have similar coordinating characteristics without having these disadvantages. We envisioned that the use of pincer ligands with sulfinyl groups as phosphine surrogates can solve these problems. Sulfoxides (mainly DMSO) are well-known as ligands in late transition metal complexes.⁷ They are air-stable (requiring harsh conditions to oxidize them to the corresponding sulfones), they can act as S or O donors according to electronic and steric requirements,^{7e,8} and they are better σ-donors than nitriles and good π-acceptors (S coordination).⁹ Despite these advantages and the vast number of known pincer complexes, sulfoxo-based pincer complexes are very scarce.¹⁰ These facts inspired us to

* To whom correspondence should be addressed. E-mail: david.milstein@weizmann.ac.il.

[†] Department of Organic Chemistry, Weizmann Institute of Science.

[‡] University of Karlsruhe.

[§] Unit of Chemical Research Support, Weizmann Institute of Science.

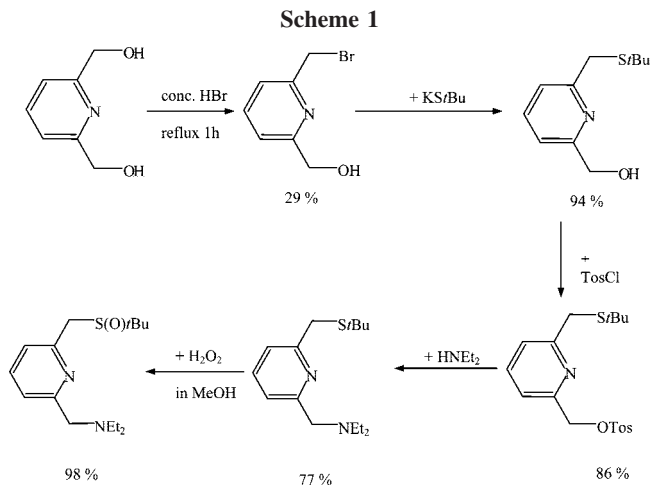
(1) Selected reviews on this topic: (a) Morales-Morales, D.; Jensen, C. M. *The Chemistry of Pincer Compounds*; Elsevier: Amsterdam, 2007. (b) Szabo, K. J. *Synlett* **2006**, 6, 811. (c) van der Boom, M. E.; Milstein, D. *Chem. Rev.* **2003**, 103, 1759. (d) Singleton, J. T. *Tetrahedron* **2003**, 59, 1837. (e) Albrecht, M.; van Koten, G. *Angew. Chem., Int. Ed.* **2001**, 40, 3750. (f) Jensen, C. M. *Chem. Commun.* **1999**, 24, 2443. (g) Rybtchinski, B.; Milstein, D. *Angew. Chem., Int. Ed.* **1999**, 38, 870.

(2) (a) Vignalok, A.; Milstein, D. *J. Am. Chem. Soc.* **1997**, 119, 7873. (b) Ohff, M.; Ohff, A.; van der Boom, M. E.; Milstein, D. *J. Am. Chem. Soc.* **1997**, 119, 11687. (d) Vignalok, A.; Uzan, O.; Shimon, L. J. W.; Ben-David, Y.; Milstein, D. *Organometallics* **1999**, 19, 895. (e) Rybtchinski, B.; Milstein, D. *Angew. Chem., Int. Ed.* **1999**, 38, 870. (f) Cohen, R.; van der Boom, M. E.; Shimon, L. J. W.; Rozenberg, H.; Milstein, D. *J. Am. Chem. Soc.* **2000**, 122, 7723. (g) Ashkenazi, N.; Vignalok, A.; Parthiban, S.; Ben-David, Y.; Shimon, L. J. W.; Martin, J. M. L.; Milstein, D. *J. Am. Chem. Soc.* **2000**, 122, 8797. (h) Cohen, R.; Rybtchinski, B.; Gandelman, M.; Shimon, L. J. W.; Martin, J. M. L.; Milstein, D. *Angew. Chem., Int. Ed.* **2003**, 42, 1949. (i) van der Boom, M. E.; Iron, M. A.; Ataolyu, O.; Shimon, L. J. W.; Rozenberg, H.; Ben-David, Y.; Konstantinovskii, L.; Martin, J. M. L.; Milstein, D. *Inorg. Chim. Acta* **2004**, 357, 1854. (j) van der Boom, M. E.; Liou, S. Y.; Shimon, L. J. W.; Ben-David, Y.; Milstein, D. *Inorg. Chim. Acta* **2004**, 357, 4015. (k) Frech, C. M.; Shimon, L. J. W.; Milstein, D. *Angew. Chem., Int. Ed.* **2005**, 44, 1709. (l) Kossov, E.; Iron, M. A.; Rybtchinski, B.; Ben-David, Y.; Shimon, L. J. W.; Konstantinovskii, L.; Martin, J. M. L.; Milstein, D. *Chem.—Eur. J.* **2005**, 11, 2319. (m) Frech, C. M.; Ben-David, Y.; Weiner, L.; Milstein, D. *J. Am. Chem. Soc.* **2006**, 128, 7128. (n) Frech, C. M.; Milstein, D. *J. Am. Chem. Soc.* **2006**, 128, 12434. (o) Frech, C. M.; Shimon, L. J. W.; Milstein, D. *Helv. Chim. Acta* **2006**, 89, 1730. (p) Salem, H.; Ben-David, Y.; Shimon, L. J. W.; Milstein, D. *Organometallics* **2006**, 25, 2292. (q) Gauvin, R. M.; Rozenberg, H.; Shimon, L. J. W.; Ben-David, Y.; Milstein, D. *Chem.—Eur. J.* **2007**, 13, 1382. (r) Montag, M.; Schwartsburd, L.; Cohen, R.; Leitus, G.; Ben-David, Y.; Martin, J. M. L.; Milstein, D. *Angew. Chem., Int. Ed.* **2007**, 46, 1901. (s) Schwartsburd, L.; Poverenov, E.; Shimon, L. J. W.; Milstein, D. *Organometallics* **2007**, 26, 2931. (t) Frech, C. M.; Shimon, L. J. W.; Milstein, D. *Chem.—Eur. J.* **2007**, 13, 7501.

(3) (a) Gandelman, M.; Vignalok, A.; Shimon, L. J. W.; Milstein, D. *Organometallics* **1997**, 16, 3981. (b) Gandelman, M.; Vignalok, A.; Konstantinovskii, L.; Milstein, D. *J. Am. Chem. Soc.* **2000**, 122, 9848. (c) Gandelman, M.; Shimon, L. J. W.; Milstein, D. *Chem.—Eur. J.* **2003**, 9, 4295. (d) Poverenov, E.; Gandelman, M.; Shimon, L. J. W.; Rozenberg, H.; Ben-David, Y.; Milstein, D. *Chem.—Eur. J.* **2004**, 10, 4673. (e) Poverenov, E.; Gandelman, M.; Shimon, L. J. W.; Rozenberg, H.; Ben-David, Y.; Milstein, D. *Organometallics* **2005**, 24, 1082. (f) Poverenov, E.; Leitus, G.; Shimon, L. J. W.; Milstein, D. *Organometallics* **2005**, 24, 5937.

(4) Rybtchinski, B.; Oevers, S.; Montag, M.; Vignalok, A.; Rozenberg, H.; Martin, J. M. L.; Milstein, D. *J. Am. Chem. Soc.* **2001**, 123, 9064.

(5) (a) Hermann, D.; Gandelman, M.; Rozenberg, H.; Shimon, L. J. W.; Milstein, D. *Organometallics* **2002**, 21, 812. (b) Ben-Ari, E.; Gandelman, M.; Rozenberg, H.; Shimon, L. J. W.; Milstein, D. *J. Am. Chem. Soc.* **2003**, 125, 4714. (c) Zhang, J.; Gandelman, M.; Shimon, L. J. W.; Rozenberg, H.; Milstein, D. *Organometallics* **2004**, 23, 4026. (d) Ben-Ari, E.; Cohen, R.; Gandelman, M.; Shimon, L. J. W.; Martin, J. M. L.; Milstein, D. *Organometallics* **2006**, 25, 3190. (e) Ben-Ari, E.; Leitus, G.; Shimon, L. J. W.; Milstein, D. *J. Am. Chem. Soc.* **2006**, 128, 15390. (f) Zhang, J.; Leitus, G.; Ben-David, Y.; Milstein, D. *Angew. Chem., Int. Ed.* **2006**, 45, 1113. (g) Feller, M.; Karton, A.; Leitus, G.; Martin, J. M. L.; Milstein, D. *J. Am. Chem. Soc.* **2006**, 128, 12400.

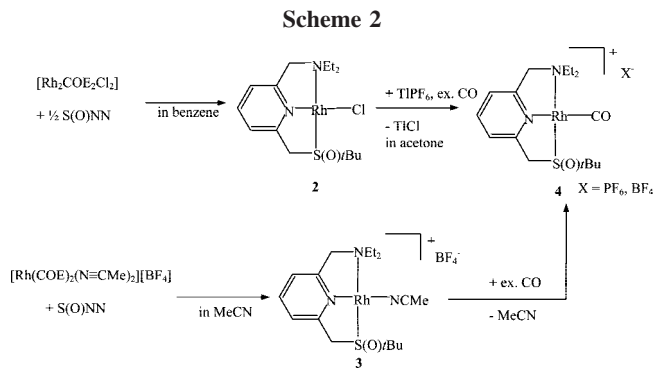


design a new, pyridine-based S(O)NN pincer ligand for the preparation of S(O)NN-Ir^I and S(O)NN-Rh^I compounds in order to study their properties and reactivity.

Results and Discussion

Ligand Synthesis. The new S(O)NN-type ligand **1** was synthesized in five steps from the commercially available pyridine-2,6-dimethanol (Scheme 1). In the first step, this compound was brominated by refluxing in concentrated HBr for 1 h. The pure 2-bromomethylpyridine-6-methanol was obtained after recrystallization from hexane/ethylacetate in 29% yield. The bromo substituent was replaced by the S *t*Bu group in nearly quantitative yield by reaction with KS *t*Bu in ethanol. The amine “arm” was then introduced in moderate yield by tosylation of the hydroxy function followed by nucleophilic substitution with a large excess of diethylamine. Finally, the S(O)NN ligand was obtained as a racemic mixture (for first studies on the reactivity of the new Ir- and Rh-S(O)NN complexes, preparation of the enantiomeric pure ligand is not needed) by oxidation with an excess of H₂O₂ in methanol following a modified protocol by Drabowicz et al.¹¹ Ligand **1** is a yellow oil, indefinitely air- and water-stable, but very hygroscopic.

Synthesis and Characterization of S(O)NN-Based Rh Complexes. Ligand **1** (dissolved in benzene) reacts cleanly with a benzene solution of Rh₂(COE)₄Cl₂ to obtain the neutral complex **2** (Scheme 2). The ¹H NMR spectrum shows two



doublets at 3.99 and 4.27 ppm for the benzylic protons of the amine arm and two high-field-shifted doublets at 4.03 and 4.83 ppm for the CH₂-S protons, which clearly indicates coordination (in the free S(O)NN ligand, the CH₂N protons are observed as a singlet at 3.77 ppm). The resonances of the CH₂-S as well as the C(CH₃)₃ carbon atoms in the ¹³C{¹H} NMR spectrum were observed as doublets with a coupling constant of 4.0 and 1.9 Hz, respectively, due to Rh couplings. IR spectroscopy is an excellent method to determine whether O or S bonding of the sulfoxide ligand occurs (O bonding: shift of the SO stretch to lower frequencies; S bonding: shift of the SO stretch to higher frequencies).^{8a} The SO stretch in **2** was detected as a strong band at 1072 cm⁻¹ compared to 1030 cm⁻¹ in noncoordinated **1**, which is in agreement with S bonding.¹² The composition of **2** was confirmed by ESI mass spectroscopy as well as elemental analysis. **2** is highly soluble in methanol, well soluble in water and acetone, and stable toward air and resists oxidation under N₂O (5 atm) even upon irradiation with UV light in an acetone solution.

The cationic Rh-S(O)NN complex **3** was formed when a solution of ligand **1** in acetonitrile was added to the *in situ* formed precursor [Rh(COE)₂(NCCH₃)₂][BF₄].^{5a,13} The 16-e complex is stabilized by one acetonitrile ligand, and the signal pattern of the S(O)NN ligand in the ¹H and ¹³C{¹H} NMR spectra of **3** is similar to the one observed for **1**. In the ¹H NMR, the coordinated CH₃CN gives rise to an additional, high-field-shifted singlet at 2.56 ppm, and in the ¹³C{¹H} NMR the nitrile carbon atom was observed as a doublet due to Rh coupling. The CN stretch can be detected at 2280 cm⁻¹, indicating *end-on* coordination, and the SO stretch of 1080 cm⁻¹ confirms S bonding.

The cationic S(O)NN-Rh carbonyl complex **4** can be obtained in two different ways: by replacing the acetonitrile ligand in **3** with CO or by chloride abstraction from **2** with TIPF₆ under an CO atmosphere (Scheme 2). In both ways, **4** was formed quantitatively when the reactions were performed in an NMR tube without workup.

The ¹H NMR spectrum of **4** shows the typical pattern for the coordinated S(O)NN ligand, and the resonance of the carbonyl carbon was detected in the ¹³C{¹H} NMR spectrum at 188.30 ppm as doublet with a coupling constant of 74.5 Hz due to coupling with the Rh atom. The CO stretch in **4** was observed at 2009 cm⁻¹, which is relatively high, compared with the cationic Rh-PNP carbonyl complex [Rh(2,6-di(diphenylphosphinomethyl)pyridine)(CO)][Cl], in which this band was observed at 1980 cm⁻¹.¹⁴ This indicates a relatively electron-poor Rh center in **4**, which is caused by the lower σ-donor ability of

(6) (a) Zhang, J.; Leitus, G.; Ben-David, Y.; Milstein, D. *J. Am. Chem. Soc.* **2005**, *127*, 10840. (b) Zhang, J.; Gandelman, M.; Herrman, D.; Leitus, G.; Shimon, L. J. W.; Ben-David, Y.; Milstein, D. *Inorg. Chim. Acta* **2006**, *359*, 1955. (c) Zhang, J.; Gandelman, M.; Shimon, L. J. W.; Milstein, D. *Dalton Trans.* **2007**, 107. (d) Gunanathan, C.; Ben-David, Y.; Milstein, D. *Science* **2007**, *317*, 790.

(7) (a) Selected reviews Davies, J. A. *Adv. Inorg. Chem. Radiochem.* **1981**, *24*, 115. (b) Kagan, H. B.; Ronan, B. *Rev. Heteroat. Chem.* **1992**, *7*, 92. (c) Kukushkin, V. Y. *Coord. Chem. Rev.* **1995**, *139*, 375. (d) Calligaris, M.; Carugo, O. *Coord. Chem. Rev.* **1996**, *153*, 83. (e) Alessio, E. *Chem. Rev.* **2004**, *104*, 4203.

(8) (a) Calligaris, M. *Coord. Chem. Rev.* **2004**, *248*, 351. (b) Li, J. R.; Bu, X. H. *Eur. J. Inorg. Chem.* Published online 2007; DOI: 10.1002/ejic.200701031.

(9) Diaz, C.; Yutronic, N. *Polyhedron* **1988**, *7*, 673.

(10) To the best of our knowledge, there are only three publications dealing with pincer sulfoxide complexes: (a) S(O)SS(O) ligands: Riley, D. P.; Oliver, J. D. *Inorg. Chem.* **1986**, *25*, 1825. (b) SS(O)S ligands: Riley, D. P.; Oliver, J. D. *Inorg. Chem.* **1986**, *25*, 1821. (c) S(O)CS(O) ligands: Evans, D. R.; Huang, M.; Seganiash, W. M.; Fettingner, J. C.; Williams, T. L. *Organometallics* **2002**, *21*, 893.

(11) Drabowicz, J.; Łyżwa, P.; Popielarczyk, M.; Mikołajczyk, M. *Synthesis* **1990**, *10*, 93.

(12) Dorta, R.; Rozenberg, H.; Milstein, D. *Chem. Commun.* **2002**, 710.

(13) Schrock, R. R.; Osborn, J. A. *J. Am. Chem. Soc.* **1971**, *93*, 3089.

(14) Vasapollo, G.; Giannoccaro, P.; Nobile, C. F.; Sacco, A. *Inorg. Chim. Acta* **1981**, *48*, 125.

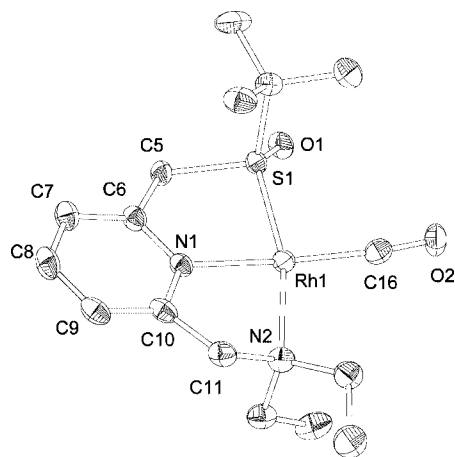


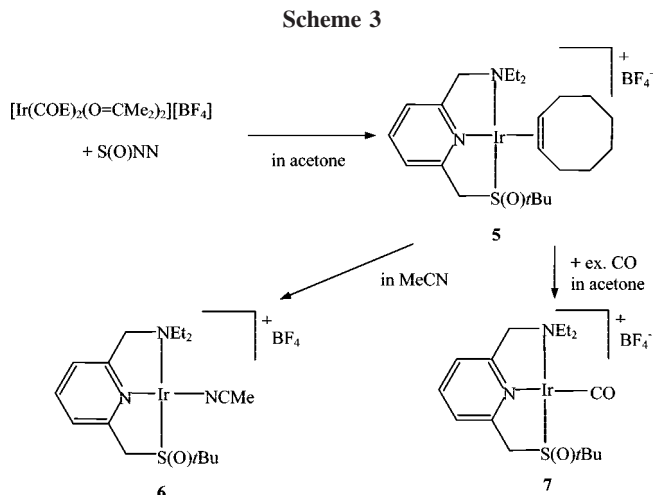
Figure 1. Thermal ellipsoid drawing of the molecular cation of $[\text{Rh}(\text{S}(\text{O})\text{NN})(\text{CO})][\text{PF}_6]$, **4** (thermal ellipsoids at 50% probability; H atoms omitted for clarity). Selected bond distances [Å] and angles [deg]: Rh1–N1 2.031(2), Rh1–N2 2.144(1), Rh1–S1 2.194(1), Rh1–C16 1.856(3), C16–O2 1.140(4), S1–O1 1.478(2), S1–C5 1.828(3), C5–C6 1.502(4), C6–C7 1.382(4), C7–C8 1.391(4), C8–C9 1.379(5), C9–C10 1.392(4), C10–N1 1.349(4), N1–C6 1.356(4), C10–C11 1.493(4), C11–N2 1.514(3); C16–Rh1–N1 175.36(11), S1–Rh1–N2 164.91(6), N1–Rh1–N2 80.03(8), S1–Rh1–N1 185.05(7), C6–C5–S1 111.13(20), C5–S1–O1 106.94(12).

the sulfinyl and amine groups compared to phosphines. The good π -acceptor ability of the CO ligand in **4** reduces the electron density on the Rh compared to **2** and **3**, which results in a stronger S donation, and due to this, the SO stretch is shifted to 1107 cm^{-1} , which is considerably higher than in **2** or **3**.

The molecular structure of **4** was confirmed by an X-ray diffraction study of yellow single crystals obtained by diffusion of pentane into an acetone solution of **4**. The rhodium atom in **4** adopts a distorted square-planar geometry involving the S(O)NN and the carbonyl ligands (Figure 1). The rhodium sulfur bond length of $2.194(1)\text{ Å}$ is in the range of other Rh^{I} sulfoxide complexes with low *trans*-influencing ligands.^{12,15} The rhodium atom is located in the S1–N1–O1–C16 plane, and no interactions with the PF_6^- counteranion are observed.

Synthesis and Characterization of S(O)NN-Based Ir Complexes. Attempts to prepare the iridium analogue of **2** by the reaction of $\text{Ir}_2(\text{COE})_4(\text{Cl})_2$ with the S(O)NN ligand failed, resulting in mixtures of noncharacterized compounds. However, reaction of the S(O)NN ligand with the cationic precursor $[\text{Ir}(\text{COE})_2(\text{O}=\text{CMe}_2)]^+[\text{BF}_4]^-$, which was not successful in the case of rhodium, yielded the cationic Ir–S(O)NN η^2 -cyclooctene complex **5** (Scheme 3).

The ^1H and $^{13}\text{C}\{^1\text{H}\}$ NMR spectra of **5** exhibit typical signal patterns of the coordinated S(O)NN ligand like in the case of the rhodium complexes **2–4**. Due to the asymmetric nature of the S(O)NN ligand, all 14 hydrogen atoms of the coordinated COE are chemically different, resulting in a relatively complex signal pattern in the ^1H NMR for this ligand. The resonances of the CH_2 protons were detected as several multiplets at 1.36 to 1.73 ppm (overlapped multiplets), 2.30 ppm, 2.67 ppm, and 3.45 ppm as well as the vinylic protons at 3.45 and 4.31 ppm in an integration ratio of 8:2:1:2:1. The ^{19}F NMR spectra show a singlet at 151.30 ppm, which is typical for a noncoordinated BF_4^- anion. The SO stretch in **5** was observed at 1098 cm^{-1} ,



confirming the expected sulfur bonding to the soft Ir^{I} center. In contrast to similar electron-rich PNP-based iridium pincer complexes, no activation of vinylic^{5a} or aromatic^{5b,d,e} C–H bonds takes place, probably as a result of the low donor ability of the S(O)NN ligand, compared to the phosphine analogues.

The COE ligand in **5** can smoothly be replaced by small ligands like acetonitrile or CO, resulting in the cationic iridium(I) complexes **6** and **7** (Scheme 3). The proton resonances of the acetonitrile ligand in **6** were observed in the ^1H NMR spectrum as a high-field-shifted (compared to free acetonitrile) singlet at 2.76 ppm, and the CN stretch was detected at 2272 cm^{-1} . The SO stretch of **5** could not be determined, because the very strong BF stretch of the BF_4^- counteranion that appears at 1055 cm^{-1} overlaps the expected area of the SO stretch (see **3**). The $^{13}\text{C}\{^1\text{H}\}$ NMR spectrum of **7** shows the resonance of the carbonyl carbon at 179.81 ppm, which is in the range of cationic Ir^{I} PNP complexes.^{5d} The CO stretch of **7** at 1991 cm^{-1} is at a significantly higher frequency than in the case of the cationic phosphine-based Ir^{I} carbonyl complex $[\text{Ir}(\text{PNP})(\text{CO})][\text{PF}_6]$ ^{5d,16} (1961 cm^{-1}), because of lower back-bonding in the former. Like in the carbonyl complex **4**, the SO stretch of **7** is relatively high shifted at 1106 cm^{-1} due to the good acceptor ability of the CO ligand, leading to an electron-poor iridium center and strong sulfur donation.

The molecular structure of **6** was confirmed by an X-ray diffraction study of yellow crystals obtained by slow diffusion of pentane into an acetone solution of **6** (Figure 2).

The iridium center of **6** adopts a distorted square-planar geometry with an S-coordinated sulfinyl group. The Ir–S distance of $2.157(28)\text{ Å}$ is comparable to the length of the Ir–S bond in the cationic Ir^{I} DMSO complex $[\text{Ir}(\text{DMSO})_2(\text{pyridine})_2][\text{PF}_6]$ ¹⁵ ($2.1870(14)\text{ Å}$), in which a nitrogen donor ligand is located *trans* to the sulfoxide.

Synthesis, Characterization, and Theoretical Investigations of Deprotonated S(O)NN-Based Rh and Ir Carbonyl Complexes. While deprotonation of a PNP-based complex, leading to dearomatization, was reported several years ago,¹⁷ the high reactivity of such species was discovered during the last three years, including iridium-mediated C–H activation reactions^{5d,e} and unique ruthenium-catalyzed esterification,^{6a} hydrogenation,^{5f} dehydrogenation,^{6c} and amidification^{6d} reactions, in which dearomatized PNP and PNN compounds are the

(15) (a) Dorta, R.; Rozenberg, H.; Shimon, L. J. W.; Milstein, D. *J. Am. Chem. Soc.* **2002**, *124*, 188. (b) Dorta, R.; Rozenberg, H.; Shimon, L. J. W.; Milstein, D. *Chem.–Eur. J.* **2003**, *9*, 5237.

(16) Kloek, S. M.; Heinekey, D. M.; Goldberg, K. I. *Organometallics* **2006**, *25*, 3007.

(17) Sacco, A.; Vasapollo, G.; Nobile, C. F.; Piergiovanni, A. *J. Organomet. Chem.* **1988**, *356*, 397.

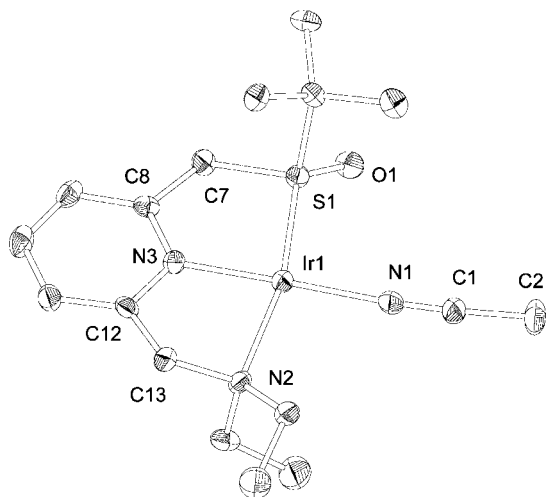
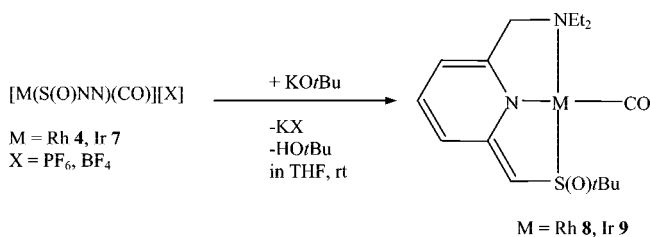


Figure 2. Thermal ellipsoid drawing of the cation of [Ir-(S(O)NN)(NCMe)][BF₄], **6** (thermal ellipsoids at 50% probability; H atoms are omitted for clarity). Selected bond distances [Å] and angles [deg]: Ir1–S1 2.157(28), Ir1–N1 1.985(8), Ir1–N2 2.155(22), Ir1–N3 1.975(7), S1–O1 1.487(5), N1–C1 1.141(8), S1–C7 1.826(8), C7–C8 1.492(9); S1–Ir1–N2 166.17(11), N1–Ir1–N3 178.07(17), S1–Ir1–N3 86.10(12), N2–Ir1–N3 80.25(14), S1–Ir1–N1 95.61(12), N1–Ir1–N2 98.08(16), S1–C7–C8 111.84(35), C7–S1–Ir1 100.41(14).

Scheme 4



active catalysts. Because protons on α -carbon atoms in sulfoxides are in general more acidic than in the corresponding phosphines, the deprotonation of an appropriate Rh- or Ir-S(O)NN precursor should be very facile and result in more robust complexes as compared with their phosphine analogues. Indeed, the cationic carbonyl complexes **4** and **7** can be deprotonated in good yields with KO*t*Bu in THF to obtain the deep red, neutral, and dearomatized compounds **8** and **9** (Scheme 4).

The ¹H NMR resonances at 5.27, 5.96, and 6.41 ppm in the spectrum of **8**, as well as 5.32, 6.00, and 6.42 ppm in the spectrum of **9** indicate dearomatization of the pyridine rings in these complexes. The two doublets for the CH₂-S protons in the precursors **4** and **7** disappeared and just one singlet with an integration of one proton at 4.13 (**8**) and 4.39 ppm (**9**), respectively, remains for the benzylic proton at the sulfinyl arm. Evidence for sp² hybridization of the benzylic carbon atoms in these arms is given by the ¹³C{¹H} NMR spectra, where these signals are high field shifted to 79.12 (**8**) and 81.32 ppm (**9**). The CO stretches of **8** (1974 cm⁻¹) and **9** (1963 cm⁻¹) are at lower frequency as compared to those observed for **4** and **7**, indicating more back-bonding in the former. Also the SO stretches are shifted to lower frequencies (1055 cm⁻¹ for **8** and 1063 cm⁻¹ for **9**) but still in the range typical for S-bonded sulfoxides. Suitable crystals for X-ray diffraction of **8** and **9** were obtained at -30 °C from saturated solutions in a toluene/pentane mixture. The molecular structures of **8** and **9** are shown in Figure 3, confirming the deprotonated nature of **8** and **9**.

The rhodium atom in **8** adopts a distorted square-planar geometry involving the S-bonded S(O)NN ligand and the carbonyl ligand and is located in the S1–N1–N2–O16 plane. The distances in the pyridine ring exhibit a slight alternation as compared with the cationic precursor **4** (Table 1), in agreement with the dearomatization observed in the corresponding ¹H and ¹³C{¹H} NMR spectra.

Importantly, the bond lengths S1–C5 (1.722(3) Å) and C5–C6 (1.391(5) Å) are drastically shortened compared to **4**, in which the corresponding distances are 1.828(5) and 1.502(4) Å, respectively. The C5–C6 bond shortening of 0.11 Å is in the same range as observed in the dearomatized PNP-based complexes [Ru(PNP*)(H)(CO)]^{5f} (0.10 Å) but significantly larger than in [Pt(PNP*)(Cl)]¹⁷ (0.7 Å). Noteworthy, the C5–S1 bond in **8** is 0.10 Å shorter than in **4**, much more than the decrease in length observed for the C–P bond of PNP complexes. The C–P bond length in [Ru(PNP*)(H)(CO)]^{5f} changes by about 0.04 Å as a result of deprotonation and in [Pt(PNP*)(Cl)]¹⁷ by about 0.06 ppm. The pyridine ring in **9** shows a very similar bond alternation to that found in **8**. The S1–C5 (1.712(7) Å) and C5–C6 (1.390(8) Å) bond lengths are also short and very close to the corresponding bond distances in **8**. The iridium atom in **9** is positioned also *in plane* and the S-coordination of the sulfinyl group was confirmed.

DFT Computational Study

To clarify the bonding situation in dearomatized **8** as compared with **4**, DFT calculations were performed at the BP/TZVPP level. To reduce the computational effort, the ethyl and *tert*-butyl groups were replaced by methyl groups, leading to the model compounds [L'HRh(CO)]⁺ (**4a**) and [L'Rh(CO)] (**8a**) (see Supporting Information for all calculated structures). For the cationic complex **4a** we calculate C–C, C–S, and S–O distances of 1.4998, 1.8644, and 1.4729 Å, respectively, while for the deprotonated form **8a**, the calculated bond lengths of interest are 1.3919 (C–C), 1.7276 (C–S), and 1.4872 Å (S–O). Thus, the experimentally observed trends are well reproduced by our calculations at that level of theory. Furthermore, we calculate some localization of the C–C bonds in the pyridine ring. Whereas the optimized pyridine C–C distances of cationic **4a** show no significant alternation, we calculate for neutral **8a** (starting from C_{ortho}) 1.4343 C(1)–C(2), 1.3758 C(2)–C(3), 1.4185 C(3)–C(4), and 1.3826 Å C(4)–C(5).

For an analysis of the bonding situation, it is instructive to preface our analysis with a short description of the bonding situation of DMSO and its anion.¹⁸ The main geometric change associated with deprotonation of DMSO is a change in the C–S bond lengths. At our level of theory, the (“methylene”) C–S bond decreases from 1.8305 Å to 1.7091 Å in the deprotonated form, whereas the C(methyl)–S distance (from 1.8305 Å to 1.8482 Å) and the S–O distance (from 1.5004 Å to 1.5466 Å) slightly increase. The DMSO anion adopts a conformation with a pyramidalized methyl carbon atom and a staggered, *gauche* arrangement of the lone pairs at the oxygen and carbon atoms. As pointed out by Streitwieser et al.,^{18a} this change in geometry does not reflect a delocalization of the negative charge to the sulfoxide moiety, but is rather due to an electrostatic stabilization of the anionic methylene carbon atom and the formally positively charged sulfur atom. The

(18) (a) Speers, P.; Laidig, K. E.; Streitwieser, A. *J. Am. Chem. Soc.* **1994**, *116*, 9257. (b) Jitariu, L. C.; Wilson, C.; Hirst, D. M. *J. Mol. Struct. (THEOCHEM)* **1997**, *391*, 111. (c) Buncel, E.; Park, K. T.; Dust, J. M.; Manderville, R. A. *J. Am. Chem. Soc.* **2003**, *125*, 5388.

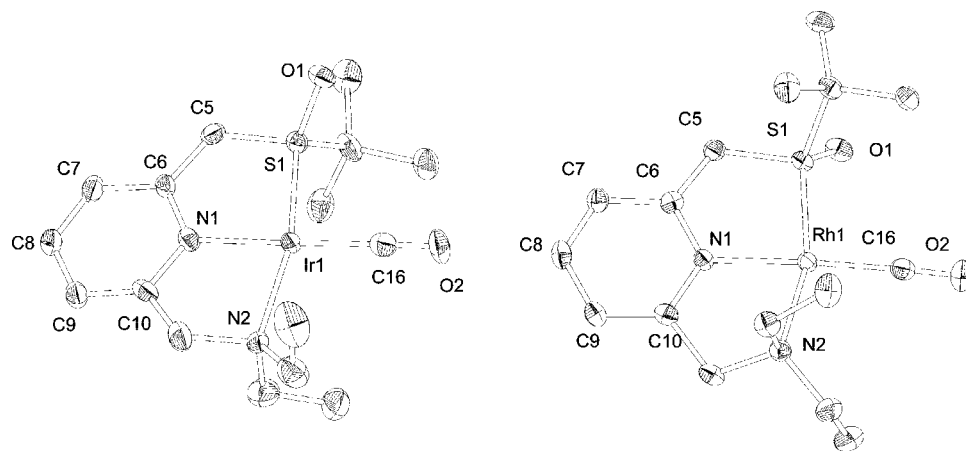


Figure 3. Thermal ellipsoid drawing of the molecular structure of [Rh(S(O)NN*)(CO)] (**8**) and [Ir(S(O)NN*)(CO)] (**9**) (thermal ellipsoids at 50% probability; H atoms omitted for clarity). Selected bond distances [Å] and angles [deg]: **1** Rh1–C16 1.850(3), Rh1–S1 2.233(1), Rh1–N1 2.017(2), Rh1–N2 2.141(2), C16–O2 1.143(4), S1–O1 1.490(2), S1–C5 1.722(3), C5–C6 1.391(5), C6–N1 1.373(4), C6–C7 1.432(4), C7–C8 1.360(5), C8–C9 1.414(4), C9–C10 1.368(4), C10–N1 1.363(4), C10–C11 1.501(4), C11–N2 1.497(4); N1–Rh1–N2 162.52(6), N1–Rh1–C16 175.69(12), S1–Rh1–N1 83.94(7), N1–Rh1–N2 79.87(9), S1–Rh1–C16 97.34(10), N2–Rh1–C16 99.29(12), C6–C5–S1 117.96(23), Rh1–S1–C5 100.67(11). **2** Ir1–S1 2.217(2), Ir1–N1 2.017(5), Ir1–N2 2.136(5), Ir1–C16 1.856(7), C16–O2 1.422(8), S1–O1 1.497(4), S1–C5 1.712(7), C5–C6 1.390(8), C6–C7 1.445(9), C7–C8 1.361(9), C8–C9 1.407(9), C9–C10 1.372(9), C10–N1 1.367(7), N1–C6 1.379(7); S1–Ir1–N2 163.45(14), N1–Ir1–C16 176.80(24), N1–Ir1–S1 84.14(13), N1–Ir1–N2 80.09(18), S1–Ir1–C16 96.75(20), N2–Ir1–C16 99.27(23), Ir1–S1–C5 101.15(22), S1–C5–C6 117.95(46).

Table 1. Comparison of the Pyridine Ring Bond Lengths in **4** and **8**

bond	cationic 4	deprotonated 8
C6–C7	1.382	1.437
C7–C8	1.391	1.369
C8–C9	1.379	1.398
C9–C10	1.392	1.377
C10–N1	1.349	1.355
N1–C6	1.356	1.369

negative charge of the anion is thus primarily localized on the methylene fragment, with a small transfer of charge to sulfur and almost no change in the population of the oxygen-centered orbitals of the DMSO anion.

Substitution of one methylene hydrogen atom of the DMSO anion with an *o*-pyridyl substituent, as found in the S(O)NN ligand **1**, has two effects on the anionic carbon atom. First, the optimized structure features an almost planar carbon atom, in which the p electron is delocalized into the π framework of the pyridine substituent. The sum of angles at the carbanionic center is 359°. As compared with the protonated species (*o*-C₅NH₄)-CH₂-S(O)Me, shortening of the C–S distance is observed (see Figure 4), similar to the corresponding change of the DMSO anion compared to DMSO, as described above.

In addition, a shortening of the C(pyridine)–C(carbanion) is observed due to delocalization of the occupied C(carbanion) p orbital into the pyridine π system. For the carbanion [(*o*-C₅NH₄)-CH-S(O)Me][−] we calculate significant alternations of the C–C

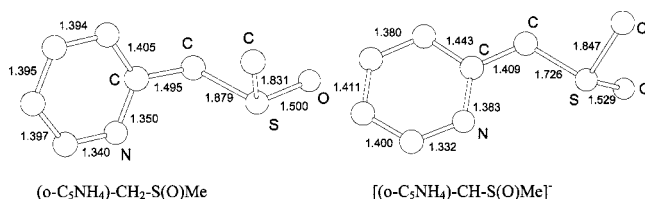


Figure 4. DFT-calculated structures of (*o*-C₅NH₄)-CH₂-S(O)Me and [(*o*-C₅NH₄)-CH-S(O)Me][−] (BP/TZVPP level) (distances in Å).

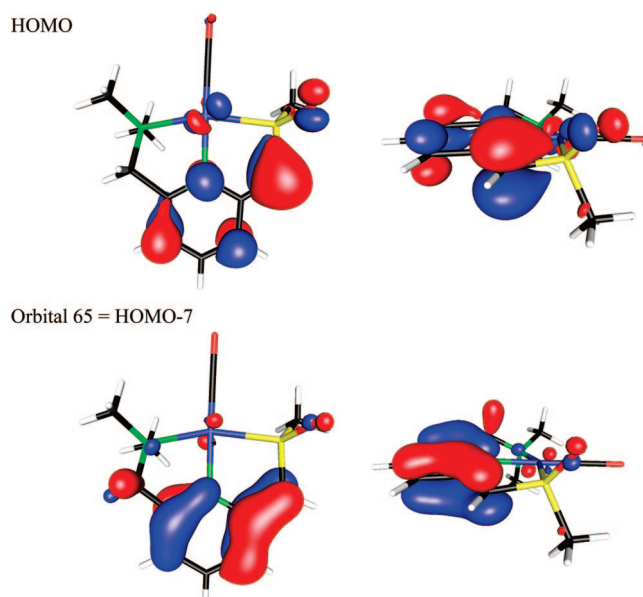
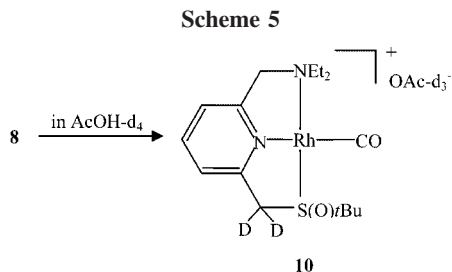


Figure 5. Relevant DFT-calculated orbitals for complex [L/Rh(CO)], **8a**, featuring a deprotonated, dearomatized S(O)NN pincer ligand.

and C–N distances within the pyridine ring.¹⁹ These main features of [(*o*-C₅NH₄)-CH-S(O)Me][−] are retained in the ligand of **8a**. Figure 5 shows the HOMO as well HOMO–7 of this complex. HOMO–7 is a ligand-centered π orbital, in this case with one nodal plane through the pyridine ring. It clearly reveals the delocalization of the occupied carbanion p orbital into the π system of the pyridine part of the ligand. The HOMO of **8a** is also mainly ligand-centered and reveals a high contribution at the benzylic carbon.

(19) The known carbanion [(*o*-C₅NH₄)-CH-S(O)Me][−] was generated *in situ* and was not structurally characterized: Ohno, A.; Higaki, M.; Okamura, M. *Heteroat. Chem.* **1992**, *3*, 513.



Protonation–Rearomatization

Complex **8** is remarkably stable toward reprotonation. No protonation occurred when a solution of **8** in toluene was treated with a 5-fold excess of methanol or when dissolved in methanol. Also, when a 10-fold excess of water was added to a solution of **8** in acetone, no reprotonation was observed even after heating overnight at 45 °C. Complete protonation to the cationic complex **10** could be achieved when **8** was dissolved in acetic acid-*d*₄, resulting in an immediate color change from deep red to orange (Scheme 5).

The ¹H NMR spectrum of **10** clearly shows the rearomatization of the pyridine ring by the presence of two doublets at 7.66 and 7.70 ppm as well as a triplet at 8.15 ppm. The benzylic protons of the S-arm disappeared because of a fast H/D exchange with the deuterated acetic acid, and the two deuterium atoms were detected in the corresponding ²D NMR spectrum as two broad singlets at 5.16 and 5.66 ppm with an integration ratio of 1:1. The ¹³C{¹H} NMR spectrum of **10** is very similar to that of **4** except for the CD₂-S carbon atom, which was observed as a quintet of doublets due to coupling with deuterium (*J* = 19 Hz) and rhodium (*J* = 4 Hz). The SO stretch in **10** was observed at 1106 cm⁻¹ and the CO stretch at 2009 cm⁻¹, as observed with **4**, confirming the cationic nature of **10**.

Further studies on the reactivity of this system as well as its application in catalysis are in progress.

Experimental Section

Computational Methods. All calculations were carried out with the DFT implementation of the TURBOMOLE program package.²⁰ The DFT calculations were performed using the BP86 functional, TZVPP basis sets, and the RI-J approximation.^{21–23} Geometry optimizations were performed without any symmetry restraints. Cartesian coordinates for geometry-optimized structures are listed in the Supporting Information. Analytic second derivatives were calculated with the module AOFORCE using the RI-J approximation.

(20) (a) Ahlrichs, R.; Bär, M.; Häser, M.; Horn, H.; Kölmel, C. *Chem. Phys. Lett.* **1989**, *162*, 165. (b) Häser, M.; Ahlrichs, R. *J. Comput. Chem.* **1989**, *10*, 104. (c) von Arnim, M.; Ahlrichs, R. *J. Comput. Chem.* **1998**, *19*, 1746. (d) von Arnim, M.; Ahlrichs, R. *J. Chem. Phys.* **1999**, *111*, 9183.

(21) (a) Becke, A. D. *Phys. Rev. A: At., Mol., Opt. Phys.* **1988**, *38*, 3098. (b) Perdew, J. P. *Rev. B: Condens. Matter Mater. Phys.* **1986**, *33*, 8822. (c) Erratum: Perdew, J. P. *Phys. Rev. B: Condens. Matter Mater. Phys.* **1986**, *34*, 7406.

(22) (a) Treutler, O.; Ahlrichs, R. *J. Chem. Phys.* **1995**, *102*, 346. (b) Eichkorn, K.; Weigend, F.; Treutler, O.; Ahlrichs, R. *Theor. Chem. Acc.* **1997**, *97*, 119. (c) Sierka, M.; Hogeckamp, A.; Ahlrichs, R. *J. Chem. Phys.* **2003**, *118*, 9136. (d) Ahlrichs, R. *Phys. Chem. Chem. Phys.* **2004**, *6*, 5119.

(23) (a) Schäfer, A.; Horn, H.; Ahlrichs, R. *J. Chem. Phys.* **1992**, *97*, 2571. (b) Schäfer, A.; Huber, C.; Ahlrichs, R. *J. Chem. Phys.* **1994**, *100*, 5829. (c) Eichkorn, K.; Treutler, O.; Öhm, H.; Häser, M.; Ahlrichs, R. *Chem. Phys. Lett.* **1995**, *242*, 652. (d) Eichkorn, K.; Weigend, F.; Treutler, O.; Ahlrichs, R. *Theor. Chem. Acc.* **1997**, *97*, 119. (e) Weigend, F.; Häser, M.; Patzelt, H.; Ahlrichs, R. *Chem. Phys. Lett.* **1998**, *294*, 143. (f) Ahlrichs, R.; May, K. *Phys. Chem. Chem. Phys.* **2000**, *2*, 943. (g) Weigend, F.; Köhn, A.; Hättig, C. *J. Chem. Phys.* **2002**, *116*, 3175. (h) Deglmann, P.; May, K.; Furche, F.; Ahlrichs, R. *Chem. Phys. Lett.* **2004**, *384*, 103. (i) Weigend, F.; Ahlrichs, R. *Phys. Chem. Chem. Phys.* **2005**, *7*, 3297.

Experimental Methods. General Procedures. All experiments were carried out under an atmosphere of purified nitrogen in an MBraun glovebox or by standard Schlenk techniques under argon. All solvents were reagent grade or better. All nondeuterated solvents were refluxed over sodium benzophenone ketyl and distilled under an argon atmosphere. Deuterated solvents were used as received. All solvents were degassed with argon and kept over molecular sieves or detergent (in case of acetone) in the glovebox. Commercially available reagents were used as received. Work with AgBF₄ was performed under the absence of light. [Rh₂(COE)₄Cl₂]²⁴ and [Ir₂(COE)₄Cl₂]²⁵ were prepared according to literature procedures. ¹H, ¹³C, ¹⁹F, and ³¹P NMR spectra were recorded on a Bruker DPX-250 or a Bruker AV-500 spectrometer. ¹³C and ³¹P NMR are broadband ¹H decoupled. NMR chemical shifts are reported in ppm downfield from tetramethylsilane (¹H, ¹³C), CCl₃F (¹⁹F), or H₃PO₄ (³¹P) and the residual solvent peak as the reference. Abbreviations used in the NMR data are as follows: s, singlet; d, doublet; dd, doublet of doublets; quint, quintet; quintd, quintet of doublets; sept, septet; m, multiplet. FT-IR spectra were recorded on a Nicolet PROTEGE 460 spectrometer. Elemental analyses were performed by H. Kolbe, Mikroanalytisches Laboratorium, 45470 Mühlheim, Germany.

2-Bromomethyl-6-pyridinemethanol. 2,6-Pyridineimethanol (15 g, 108 mmol) was refluxed in HBr (48% in water) for 1 h. After cooling to 0 °C, an ice cold, saturated NaOH solution was carefully added until pH = 14 was reached. The product was immediately extracted with 4 × 100 mL of CH₂Cl₂, and the combined organic layers were dried over MgSO₄. All volatiles were removed *in vacuo* to give the slightly pink crude product. The pure 1-bromomethyl-6-pyridinemethanol was obtained by recrystallization from hexane/ethylacetate (5:1). Yield: 6.26 g (28.7%), white, microcrystalline solid. ¹H NMR (CDCl₃, 250 MHz, 25 °C): δ 3.93 (s, br, 1 H, OH), 4.54 (s, 2 H, CH₂Br), 4.76 (s, 2 H, CH₂OH), 7.10 (d, 1 H, ³J_{HH} = 7.7 Hz, aryl-H₅), 7.34 (d, 1 H, ³J_{HH} = 7.6 Hz, aryl-H₃), 7.69 (t, 1 H, ³J_{HH} = 7.7 Hz, aryl-H₄). ¹³C{¹H} NMR (CDCl₃, 63 MHz, 25 °C): δ 33.44 (CH₂Br), 63.98 (CH₂OH), 119.89 (aryl-C₃), 122.09 (aryl-C₅), 137.76 (aryl-C₄), 155.72 (aryl-C₂), 159.21 (aryl-C₆).

2-(2-Methyl-2-propanethiomethyl)-6-pyridinemethanol. Potassium (1.22 g, 31.2 mmol) was dissolved in 50 mL of ethanol at 0 °C. 2-Methyl-2-propanthiol (3.50 mL, 31.2 mmol) was added, and the mixture was stirred for 20 min and added to a solution of 1-bromomethyl-6-pyridinemethanol (6.26 g, 31.2 mmol) in 50 mL of ethanol. The reaction mixture was heated under reflux for 2 h. All volatiles were removed *in vacuo*, 150 mL of water was added, and the product was extracted with 300 mL of CH₂Cl₂ and dried over Na₂SO₄. All volatiles were removed *in vacuo* to obtain the pure 2-(2-methyl-2-propanethiomethyl)-6-pyridinemethanol as a light yellow oil. Yield: 6.2 g (94.0%). ¹H NMR (CDCl₃, 250 MHz, 25 °C): δ 1.33 (s, 9 H, CH₃), 3.90 (s, 2 H, CH₂S), 4.51 (s, br, 1 H, OH), 4.73 (s, 2 H, CH₂OH), 7.15 (d, 1 H, ³J_{HH} = 7.7 Hz, aryl-H₃), 7.32 (d, 1 H, ³J_{HH} = 7.6 Hz, aryl-H₅), 7.62 (d, 1 H, ³J_{HH} = 7.7 Hz, aryl-H₄). ¹³C{¹H} NMR (CDCl₃, 63 MHz, 25 °C): δ 30.87 (CH₃), 35.18 (CH₂S), 43.08 (C(CH₃)₃), 64.03 (CH₂OH), 118.51 (aryl-C₃), 121.77 (aryl-C₅), 137.23 (aryl-C₄), 158.14 (aryl-C₂), 158.77 (aryl-C₆).

(24) Hofmann, P.; Meier, C.; Englert, U.; Schmidt, U. *Chem. Ber.* **1992**, *125*, 353.

(25) van der Ent, A.; Onderlinden, A. L. *Inorg. Synth.* **1990**, *28*, 90.

2-(2-Methyl-2-propanethiomethyl)-6-pyridinemethanol tosylate. 2-(2-Methyl-2-propanethiomethyl)-6-pyridinemethanol (6.20 g, 29.3 mmol) and NaOH (11.8 g, 294 mmol) was dissolved in a mixture of 220 mL of THF and 220 mL of water. A solution of *p*-toluenesulfonyl chloride (11.2 g, 58.7 mmol) in 200 mL of THF was added dropwise at 0 °C, and the reaction mixture was stirred for 4 h at room temperature. Then 200 mL water was added and the product was extracted two times with 150 mL of CH₂Cl₂. The combined organic phases were washed with 200 mL of water and dried over Na₂SO₄, and all volatiles were removed *in vacuo* to yield 8.60 g (85.9%) as a yellow oil. ¹H NMR (CDCl₃, 250 MHz, 25 °C): δ 1.32 (s, 9 H, C(CH₃)₃), 2.44 (s, 3 H, aryl-CH₃), 3.83 (s, 2 H, CH₂S), 5.11 (s, 2 H, CH₂O), 7.25 (d, 1 H, ³J_{HH} = 7.7 Hz, aryl-H₃), 7.34 (d, 2 H, ³J_{HH} = 8.0 Hz, aryl-H_m), 7.35 (d, 1 H, ³J_{HH} = 7.5 Hz, aryl-H₅), 7.63 (t, 1 H, ³J_{HH} = 7.8 Hz, aryl-H₄), 7.82 (d, 2 H, ³J_{HH} = 8.3 Hz, aryl-H₆). ¹³C{¹H} NMR (CDCl₃, 63 MHz, 25 °C): δ 21.61 (aryl-CH₃), 30.85 (C(CH₃)₃), 35.24 (CH₂S), 43.12 (C(CH₃)₃), 71.70 (CH₂O), 119.61 (aryl-C₄), 122.88 (aryl-C₃), 128.03 (aryl-C_m), 129.86 (aryl-C₆), 132.71 (aryl-C_p), 137.38 (aryl-C₅), 144.97 (aryl-C_i), 153.07 (aryl-C₂), 158.91 (aryl-C₆).

2-(2-Methyl-2-propanethiomethyl)-6-(diethylaminomethyl)pyridine. A solution of 2-(2-methyl-2-propanethiomethyl)-6-pyridinemethanol tosylate (8.60 g, 23.5 mmol) in 80 mL of THF was added dropwise at 0 °C to a stirred solution of diethylamine (40 mL) and THF (80 mL). After complete addition, the reaction mixture was stirred overnight at room temperature and all volatiles were removed *in vacuo*. The product was extracted from the oily residue with 300 mL of diethyl ether. The organic phase was washed with 100 mL of 10% aqueous NaOH solution and dried over Na₂SO₄, and all volatiles were removed *in vacuo* to yield 4.8 g (76.6%) as an orange oil. ¹H NMR (CDCl₃, 250 MHz, 25 °C): δ 1.04 (t, 6 H, ³J_{HH} = 7.1 Hz, CH₂CH₃), 1.33 (s, 9 H, C(CH₃)₃), 2.57 (q, 4 H, ³J_{HH} = 7.1 Hz, CH₂CH₃), 3.71 (s, 2 H, SCH₂), 3.91 (s, 2 H, CH₂N), 7.28 (d, 1 H, ³J_{HH} = 7.6 Hz, aryl-H₃), 7.34 (d, 1 H, ³J_{HH} = 7.6 Hz, aryl-H₅), 7.58 (t, 1 H, ³J_{HH} = 7.6 Hz, aryl-H₄). ¹³C{¹H} NMR (CDCl₃, 63 MHz, 25 °C): δ 11.87 (CH₂CH₃), 31.15 (C(CH₃)₃), 37.25 (CH₂S), 42.85 (C(CH₃)₃), 47.22 (NCH₂CH₃), 64.00 (CH₂N), 120.49 (aryl-C₂), 121.10 (aryl-C₅), 136.91 (aryl-C₄), 158.08 (aryl-C₂), 160.06 (aryl-C₆).

S(O)NN (1). 2-(2-Methyl-2-propanethiomethyl)-6-(diethylaminomethyl)pyridine (4.8 g, 18.0 mmol) was dissolved in 42 mL of methanol, and 1.30 g of HCl (37% in H₂O, 36.1 mmol) was added slowly. Then 5.2 mL of a 2-propanol/H₂SO₄ mixture (1.38 g of conc. H₂SO₄ dissolved in 38 mL of 2-propanol) and H₂O₂ (30% in H₂O, 4.7 g) were added, and the reaction solution was stirred at room temperature for 4 h. After complete reaction, solid NaOH (1.6 g, 40.6 mmol) was added in small portions and 100 mL of water was added. The product was extracted two times with 150 mL of CHCl₃, the combined organic layers were dried over Na₂SO₄, and all volatiles were removed *in vacuo*. The product was then dried for 24 h under high vacuum to remove last traces of water to yield 5.0 g (98.3%) as a viscous, yellow oil. ¹H NMR (CDCl₃, 250 MHz, 25 °C): δ 1.06 (t, 6 H, ³J_{HH} = 7.1 Hz, CH₂CH₃), 1.33 (s, 9 H, C(CH₃)₃), 2.58 (q, 4 H, ³J_{HH} = 7.1 Hz, CH₂CH₃), 3.77 (s, 2 H, CH₂N), 3.79 (d, 1 H, ²J_{HH} = 12.5 Hz, CH₂S), 4.03 (d, 1 H, ²J_{HH} = 12.5 Hz, CH₂S), 7.28 (d, 1 H, ³J_{HH} = 7.5 Hz, aryl-H₅), 7.45 (d, 1 H, ³J_{HH} = 7.8 Hz, aryl-H₃), 7.64 (t, 1 H, ³J_{HH} = 7.7 Hz, aryl-H₄). ¹³C{¹H} NMR (CDCl₃, 63 MHz, 25 °C): δ 11.76 (CH₂CH₃), 22.90 (C(CH₃)₃), 47.19 (CH₂CH₃), 53.79 (C(CH₃)₃), 54.85 (CH₂N), 59.26 (CH₂S), 121.68 (aryl-C₅), 123.01 (aryl-C₃), 136.74 (aryl-C₄), 151.40 (aryl-C₆), 160.97 (aryl-C₂). ESI-MS (*m/z*): 283.58

(100) [M + H]⁺. IR (thin film): ν [cm⁻¹] 749 (w), 808 (w), 1030 (vs, ν_{SO}), 1166 (m), 1268 (s), 1370 (m), 1464 (s), 1591 (m), 2800 (w), 2868 (m), 2928 (m), 2970 (s), 3064 (w).

[Rh(S(O)NN)Cl] (2). A solution of S(O)NN (160 mg, 0.57 mmol) in 3 mL of benzene was slowly added at room temperature to a stirred solution of [Rh₂(COE)₄(Cl)₂] (200 mg, 0.28 mmol) in 8 mL of benzene. The color changed immediately to deep red and a dark residue precipitated. The reaction mixture was stirred for an additional 2 h at room temperature, and afterward, 15 mL of pentane was added. The precipitate was filtered off and washed with 10 mL of pentane, and the product was extracted with 10 mL of methanol. All volatiles were removed *in vacuo*, and the product was washed with 15 mL of diethyl ether and dried *in vacuo* to yield 191 mg (79.6%) as an orange powder. Anal. Calcd (%) for C₁₅H₂₆NSOClRh·H₂O (438.83): C 41.06, H 6.43, N 6.38. Found: C 40.42, H 6.30, N 6.10. ¹H NMR (CD₃OD, 500 MHz, 25 °C): δ 1.47 (s, 9 H, C(CH₃)₃), 1.57 (t, 3 H, ³J_{HH} = 7.1 Hz, CH₂CH₃), 1.63 (t, 3 H, ³J_{HH} = 7.0 Hz, CH₂CH₃), 2.65 (m, 1 H, NCH₂CH₃), 2.75 (m, 1 H, NCH₂CH₃), 3.09 (m, 1 H, NCH₂CH₃), 3.19 (m, 1 H, NCH₂CH₃), 3.99 (d, 1 H, ²J_{HH} = 16.9 Hz, CH₂N), 4.03 (d, 1 H, ²J_{HH} = 17.5 Hz, CH₂S), 4.27 (d, 1 H, ²J_{HH} = 16.8 Hz, CH₂N), 4.83 (d, 1 H, ²J_{HH} = 17.4 Hz, CH₂S), 7.23 (m, 2 H, aryl-H_{3,5}), 7.75 (t, 1 H, ³J_{HH} = 7.8 Hz, aryl-H₄). ¹³C{¹H} NMR (CD₃OD, 126 MHz, 25 °C): δ 11.63 (CH₂CH₃), 11.89 (CH₂CH₃), 22.44 (C(CH₃)₃), 53.79 (CH₂CH₃), 55.42 (CH₂CH₃), 62.99 (d, ²J_{RhC} = 1.9 Hz, C(CH₃)₃), 63.49 (CH₂N), 65.49 (d, ²J_{RhC} = 4.0 Hz, CH₂S), 118.56 (aryl-C₅), 119.04 (aryl-C₃), 133.32 (aryl-C₄), 154.53 (aryl-C₂), 160.93 (aryl-C₆). ESI-MS (*m/z*): 419.61 (100) [M]⁺. IR (thin film): ν [cm⁻¹] 791 (w), 1021 (m), 1072 (vs, ν_{SO}), 1174 (m), 1260 (m), 1362 (m), 1472 (s), 2919 (m), 2961 (s), 3063 (w).

[Rh(S(O)NN)(N≡C-Me)][BF₄] (3). Rh₂COE₄Cl₂ (30 mg, 0.042 mmol) was suspended in 4 mL of acetonitrile, and AgBF₄ (15.5 mg, 0.084 mmol) in 2 mL of acetonitrile was added at room temperature. The mixture was stirred for 15 min and then filtered over cotton/Celite. The yellow filtrate was added to S(O)NN (23.1 mg, 0.084 mmol), and the mixture was stirred at room temperature for 2 h (orange solution). All volatiles were removed *in vacuo*, and the residue was washed two times with 10 mL of diethyl ether. The product was dried *in vacuo* to yield 33 mg (76.2%) of a yellow powder. Anal. Calcd (%) for C₁₇H₂₉N₃SOBF₄Rh (513.22): C 39.79, H 5.70, N 8.19. Found: C 39.71, H 5.75, N 8.17. ¹H NMR (acetone-*d*₆, 500 MHz, 25 °C): δ 1.44 (s, 9 H, C(CH₃)₃), 1.61 (t, 3 H, ³J_{HH} = 7.2 Hz, CH₂CH₃), 1.66 (t, 3 H, ³J_{HH} = 7.1 Hz, CH₂CH₃), 2.56 (s, 3 H, N⁺C-CH₃), 2.86 (m, 1 H, CH₂CH₃), 2.99 (m, 2 H, CH₂CH₃), 3.23 (m, 1 H, CH₂CH₃), 4.16 (d, 1 H, ²J_{HH} = 16.6 Hz, CH₂N), 4.35 (d, 1 H, ²J_{HH} = 17.6 Hz, CH₂S), 4.58 (d, 1 H, ²J_{HH} = 16.6 Hz, CH₂N), 5.16 (d, 1 H, ²J_{HH} = 17.6 Hz, CH₂S), 7.45 (m, 2 H, aryl-H_{3,5}), 7.93 (t, 1 H, ³J_{HH} = 7.8 Hz, aryl-H₄). ¹³C{¹H} NMR (acetone-*d*₆, 126 MHz, 25 °C): δ 2.44 (N≡C-CH₃), 11.40 (CH₂CH₃), 12.60 (CH₂CH₃), 22.46 (C(CH₃)₃), 53.36 (CH₂CH₃), 55.62 (CH₂CH₃), 63.10 (d, ²J_{RhC} = 2.3 Hz, C(CH₃)₃), 63.87 (CH₂N), 64.95 (d, ²J_{RhC} = 4.4 Hz, CH₂S), 119.42 (aryl-C₅), 120.14 (aryl-C₃), 125.52 (d, ²J_{RhC} = 10.7 Hz, N≡C-CH₃), 136.75 (aryl-C₄), 156.09 (aryl-C₆), 161.45 (aryl-C₂). ¹⁹F NMR (acetone-*d*₆, 235 MHz, 25 °C): δ 151.47 (s, 1 F, BF₄). ESI-MS (*m/z*): 426.88 (100) [Rh(S(O)NN)(N≡C-CH₃)]⁺, 87.23 (100) [BF₄]⁻. IR (thin film): ν [cm⁻¹] 783 (w), 791 (w), 1055 (vs, ν_{BF}), 1080 (s, ν_{SO}), 1174 (m), 1293 (w), 1361 (s), 1387 (m), 1463 (s), 1566 (w), 1608 (w), 2280 (w, ν_{CN}), 2868 (m), 2936 (m), 2978 (s), 3072 (w).

[Rh(S(O)NN)(CO)][PF₆] (**4**). Rh(S(O)NN)Cl (**1**) (50 mg, 0.12 mmol) and TlPF₆ (42 mg, 0.12 mmol) were dissolved in 5 mL of acetone and stirred for 1 h under nitrogen, whereby a slightly turbid, yellow solution was formed. Then 40 mL of CO was bubbled through the reaction mixture over a period of 2 min, and a yellow suspension (fine TiCl₄ precipitate) was obtained. All volatiles were removed *in vacuo* (in order to obtain a better filterable TiCl₄), and the product was extracted with 5 mL of acetone. All volatiles were removed *in vacuo*, and the residue was washed with 10 mL of diethyl ether and dried *in vacuo* to obtain 56 mg of an orange powder (83.3% yield). Suitable crystals for X-ray diffraction were grown by layering a solution of **4** in acetone with pentane at room temperature. Anal. Calcd (%) for C₁₆H₂₆N₂SO₂PF₆Rh (558.33): C 34.42, H 4.69, N 5.02. Found: C 34.38, H 4.72, N 4.88. ¹H NMR (acetone-*d*₆, 500 MHz, 25 °C): δ 1.50 (s, 9 H, C(CH₃)₃), 1.61 (t, 3 H, ³J_{HH} = 7.3 Hz, CH₂CH₃), 7.64 (t, 3 H, ³J_{HH} = 7.0 Hz, CH₂CH₃), 3.17 (m, 1 H, CH₂CH₃), 3.26 (m, 2 H, CH₂CH₃), 3.47 (m, 1 H, CH₂CH₃), 4.49 (d, 1 H, ²J_{HH} = 17.0, CH₂N), 4.90 (d, 1 H, ²J_{HH} = 16.8, CH₂N), 5.08 (d, 1 H, ²J_{HH} = 17.6 Hz, CH₂S), 5.73 (d, 1 H, ²J_{HH} = 17.6 Hz, CH₂S), 7.73 (d, 2 H, ³J_{HH} = 7.9 Hz, aryl-*H*_{3,5}), 8.21 (t, 1 H, ³J_{HH} = 7.9 Hz, aryl-*H*₄). ¹³C{¹H} NMR (acetone-*d*₆, 126 MHz, 25 °C): δ 12.10 (CH₂CH₃), 13.45 (CH₂CH₃), 22.40 (C(CH₃)₃), 56.61 (CH₂CH₃), 57.28 (CH₂CH₃), 64.8 (d, ²J_{RhC} = 2.1 Hz, C(CH₃)₃), 65.32 (CH₂S, CH₂N), 120.73 (aryl-C₅), 121.30 (aryl-C₃), 142.00 (aryl-C₄), 155.99 (aryl-C₆), 162.16 (aryl-C₂), 188.30 (d, ¹J_{RhC} = 74.5 Hz, CO). ³¹P NMR (acetone-*d*₆, 101 MHz, 25 °C): δ -143.66 (sept, 1 P, ¹J_{FP} = 707.5 Hz, PF₆). ESI-MS (*m/z*): 413.80 (100) [Rh(S(O)NN)(CO)]⁺, 87.23 (100) [BF₄]⁻. IR (thin film): ν [cm⁻¹] 843 (vs, ν_{PF}), 1057 (w), 1107 (s, ν_{SO}), 1174 (m), 1251 (w), 1396 (m), 1472 (s), 1566 (w), 1600 (m), 1693 (s), 2009 (vs, ν_{CO}), 2877 (w), 2928 (m), 2970 (m), 3098 (w).

X-ray Structural Analysis of X. Crystal Data. C₁₆H₂₆F₆N₂O₂PRhS, yellow prisms, 0.50 × 0.12 × 0.12 mm³, monoclinic, *P*2₁/*c*, *a* = 9.4640(2) Å, *b* = 16.1500(5) Å, *c* = 14.4660(4) Å, β = 106.126(1)° from 25° of data, *T* = 120(2) K, *V* = 2124.0(1) Å³, *Z* = 4, *fw* = 558.33, *D_c* = 1.746 Mg/m³, μ = 1.044 mm⁻¹.

Data Collection and Processing. Nonius KappaCCD diffractometer, Mo Kα (λ = 0.71073 Å), graphite monochromator, -12 ≤ *h* ≤ 12, -20 ≤ *k* ≤ 18, -18 ≤ *l* ≤ 18, frame scan width = 1.0°, scan speed 1.0° per 20 s, typical peak mosaicity 0.477°, 15 900 reflection collected, 5031 independent reflections (*R*_{int} = 0.071). The data were processed with Denzo-Scalepack.

Solution and Refinement. Structure solved by Patterson method with SHELXS-97. Full matrix least-squares refinement based on *F*² with SHELXL-97; 267 parameters with no restraints, final *R*₁ = 0.0356 (based on *F*²) for data with *I* > 2σ(*I*) and, *R*₁ = 0.0516 on 4846 reflections, goodness-of-fit on *F*² = 1.088, largest electron density peak = 1.271 e Å⁻³.

[Ir(S(O)NN)(η²-C₈H₁₄)] [BF₄] (**5**). Ir₂(COE)₄Cl₂ (30.0 mg, 0.033 mmol) and AgBF₄ (12.8 mg, 0.066 mg) were dissolved in 5 mL of acetone, and the mixture was stirred at room temperature for 30 min. The white precipitate (AgCl) was removed by filtration over cotton/Celite, and the solution was added to S(O)NN (19.0 mg, 0.066 mmol). The reaction mixture was stirred at room temperature for 2 h, and all volatiles were removed *in vacuo*. The orange residue was suspended in 10 mL of diethyl ether, filtered, washed with 5 mL of diethyl ether, and dried *in vacuo* to yield 37 mg (83.3%) of an orange powder. Anal. Calcd (%) for C₂₃H₄₀N₂SOIrBF₄·H₂O (689.69): C 40.05, H 6.14, N 4.06. Found: C 39.80, H 6.01, N 4.06. ¹H NMR (acetone-*d*₆, 500 MHz, 25 °C): δ 1.11 (t, 3 H, ³J_{HH} = 7.2 Hz,

CH₂CH₃), 1.25 (s, 9 H, C(CH₃)₃), 1.36–1.73 (m, 8 H, COE-CH₂), 1.81 (t, 3 H, ³J_{HH} = 7.0 Hz, CH₂CH₃), 2.30 (m, 2 H, COE-CH₂), 2.67 (m, 1 H, COE-CH₂), 2.92 (m, 1 H, CH₂CH₃), 2.99 (m, 1 H, CH₂CH₃), 3.14 (m, 2 H, CH₂CH₃), 3.45 (m, 2 H, COE-CH₂, COE-CH), 4.31 (m, 1 H, COE-CH), 4.40 (d, 1 H, ²J_{HH} = 17.0 Hz, CH₂S), 4.71 (d, 1 H, ²J_{HH} = 16.7 Hz, CH₂N), 4.93 (d, 1 H, ²J_{HH} = 16.7 Hz, CH₂N), 5.51 (d, 1 H, ²J_{HH} = 17.0 Hz, CH₂S), 7.85 (d, 1 H, ³J_{HH} = 8.5 Hz, aryl-*H*₅), 7.89 (d, 1 H, ³J_{HH} = 8.0 Hz, aryl-*H*₃), 8.36 (t, 1 H, ³J_{HH} = 7.9 Hz, aryl-*H*₄). ¹³C{¹H} NMR (acetone-*d*₆, 126 MHz, 25 °C): δ 11.91 (CH₂CH₃), 12.34 (CH₂CH₃), 24.53 (C(CH₃)₃), 25.99 (COE-CH₂), 26.41 (COE-CH₂), 30.02 (COE-CH₂), 30.17 (COE-CH₂), 30.84 (COE-CH₂), 31.69 (COE-CH₂), 55.62 (CH₂CH₃), 58.21 (CH₂CH₃), 61.10 (br, COE-CH), 65.71 (CH₂N), 66.62 (CH₂S), 67.56 (C(CH₃)₃), 82.30 (COE-CH), 119.58 (aryl-C₅), 120.05 (aryl-C₃), 141.32 (aryl-C₄), 156.86 (aryl-C₆), 162.70 (aryl-C₂). ¹⁹F NMR (acetone-*d*₆, 235 MHz, 25 °C): δ 151.30 (s, 4 F, BF₄). ESI-MS (*m/z*): 586.07 (100) [Ir(S(O)NN)(η²-C₈H₁₄)]⁺, 475.86 (12) [Ir(S(O)NN)]⁺, 87.17 (100) [BF₄]⁻. IR (thin film): ν [cm⁻¹] 1047 (vs, ν_{BF}), 1098 (s, ν_{SO}), 1166 (m), 1260 (w), 1353 (m), 1387 (w), 1481 (m), 1600 (w), 2860 (m), 2919 (s), 2987 (m), 3098 (w).

[Ir(S(O)NN)(N≡C-Me)] [BF₄] (**6**). [Ir(S(O)NN)(η²-C₈H₁₄)] [BF₄] (133.0 mg, 0.19 mmol) was dissolved in 5 mL of acetonitrile, and the mixture was stirred overnight at room temperature as a deep yellow solution was formed. A small amount of precipitate was removed by filtration over cotton/Celite, and the volatiles of the filtrate were removed *in vacuo*. The residue was washed two times with 10 mL of diethyl ether and dried *in vacuo* to yield 92 mg (80.5%) of a yellow powder. Crystals suitable for X-ray diffraction were grown by slow diffusion of pentane in an acetone solution of **6** at room temperature. ¹H NMR (acetone-*d*₆, 500 MHz, 25 °C): δ 1.33 (s, 9 H, C(CH₃)₃), 1.49 (t, 3 H, ³J_{HH} = 7.2 Hz, CH₂CH₃), 1.56 (t, 3 H, ³J_{HH} = 7.2 Hz, CH₂CH₃), 2.76 (s, 2 H, N≡C-CH₃), 3.07 (m, 1 H, CH₂CH₃), 3.17 (m, 2 H, CH₂CH₃), 3.44 (m, 1 H, CH₂CH₃), 3.85 (d, 1 H, ²J_{HH} = 17.7 Hz, CH₂S), 4.30 (d, 1 H, ²J_{HH} = 16.4 Hz, CH₂N), 4.30 (d, 1 H, ²J_{HH} = 16.5 Hz, CH₂N), 5.03 (d, 1 H, ²J_{HH} = 17.7 Hz, CH₂S), 7.41 (m, 2 H, aryl-*H*_{3,5}), 8.08 (t, 1 H, ³J_{HH} = 7.88 Hz, aryl-*H*₄). ¹³C{¹H} NMR (acetone-*d*₆, 126 MHz, 25 °C): δ 2.80 (N≡C-CH₃), 10.82 (CH₂CH₃), 12.04 (CH₂CH₃), 22.03 (C(CH₃)₃), 54.19 (CH₂CH₃), 56.71 (CH₂CH₃), 64.53 (C(CH₃)₃), 65.57 (CH₂N), 65.60 (CH₂S), 119.56 (aryl-C₅), 120.50 (aryl-C₃), 123.69 (N≡C-CH₃), 135.20 (aryl-C₄), 157.17 (aryl-C₆), 160.83 (aryl-C₂). ¹⁹F NMR (acetone-*d*₆, 235 MHz, 25 °C): δ 151.31 (s, 4 F, BF₄). IR (thin film): ν [cm⁻¹] = 1055 (vs, ν_{BF}), 1165 (m), 1285 (w), 1370 (s), 1387 (m), 1489 (s), 1600 (w), 1693 (s), 2272 (w, ν_{CN}), 2919 (m), 2970 (s), 3089 (w).

X-ray Structural Analysis of X. Crystal Data. C₁₇H₂₉BF₄N₃OIrS, yellow prisms, 0.3 × 0.3 × 0.1 mm³, monoclinic, *P*2₁/*c*, *a* = 10.7221(2) Å, *b* = 16.832(3) Å, *c* = 11.867(2) Å, β = 91.74(3)° from 20° of data, *T* = 120(2) K, *V* = 2140.7(7) Å³, *Z* = 4, *fw* = 602.50, *D_c* = 1.869 Mg/m³, μ = 6.381 mm⁻¹.

Data Collection and Processing. Nonius KappaCCD diffractometer, Mo Kα (λ = 0.71073 Å), graphite monochromator, -14 ≤ *h* ≤ 14, 0 ≤ *k* ≤ 22, 0 ≤ *l* ≤ 16, frame scan width = 1.0°, scan speed 1.0° per 50 s, typical peak mosaicity 0.989°, 30 659 reflections collected, 5684 independent reflections (*R*_{int} = 0.069). The data were processed with Denzo-Scalepack.

Solution and Refinement. Structure solved by Patterson method with SHELXS-97. Full matrix least-squares refinement based on *F*² with SHELXL-97; 259 parameters with no restraints, final *R*₁ = 0.0385 (based on *F*²) for data with *I* >

$2\sigma(I)$ and, $R_1 = 0.0564$ on 5487 reflections, goodness-of-fit on $F^2 = 1.088$, largest electron density peak = $2.149 \text{ e } \text{Å}^{-3}$, deepest hole = $-2.470 \text{ e } \text{Å}^{-3}$.

[Ir(S(O)NN)(CO)][BF₄] (7). [Ir(S(O)NN)(η^2 -C₈H₁₄)] [BF₄] (77.0 mg, 0.11 mmol) was dissolved in 5 mL of acetone, and 20 mL of CO was bubbled slowly through as the color changed to yellow. All volatiles were removed *in vacuo*, and the residue was washed with 10 mL of diethyl ether. The product was dried *in vacuo* to yield 57 mg (88.2%) of a yellow powder. Anal. Calcd (%) for C₁₆H₂₆N₂SO₂BF₄Ir (589.49): C 32.60, H 4.45, N 4.74. Found: C 32.62, H 4.37, N 4.45. ¹H NMR (acetone-*d*₆, 500 MHz, 25 °C): δ 1.49 (s, 9 H, C(CH₃)₃), 1.59 (t, 3 H, ³J_{HH} = 7.2 Hz, CH₂CH₃), 1.64 (t, 3 H, ³J_{HH} = 7.2 Hz, CH₂CH₃), 3.48 (q, 2 H, ³J_{HH} = 7.1 Hz, CH₂CH₃), 3.61 (m, 1 H, CH₂CH₃), 3.70 (m, 1 H, CH₂CH₃), 4.87 (d, 1 H, ²J_{HH} = 16.9 Hz, CH₂N), 4.97 (d, 1 H, ²J_{HH} = 17.7 Hz, CH₂S), 5.05 (d, 1 H, ²J_{HH} = 16.9 Hz, CH₂N), 5.89 (d, 1 H, ²J_{HH} = 17.7 Hz, CH₂S), 7.88 (d, 2 H, ³J_{HH} = 7.9 Hz, aryl-H_{3,5}), 8.32 (t, 1 H, ³J_{HH} = 7.9 Hz, aryl-H₄). ¹³C{¹H} NMR (acetone-*d*₆, 126 MHz, 25 °C): δ 11.81 (CH₂ CH₃), 13.07 (CH₂CH₃), 22.27 (C(CH₃)₃), 58.38 (CH₂CH₃), 58.87 (CH₂CH₃), 65.26 (CH₂N), 65.70 (C(CH₃)₃), 66.40 (CH₂N), 120.88 (aryl-C₅), 121.49 (aryl-C₃), 142.43 (aryl-C₄), 157.48 (aryl-C₆), 162.57 (aryl-C₂), 179.81 (CO). ¹⁹F NMR (acetone-*d*₆, 235 MHz, 25 °C): δ 151.45 (s, 4 F, BF₄). ESI-MS (*m/z*): 504.02 (100) [Ir(S(O)NN)(CO)]⁺, 87.23 (100) [BF₄]⁻. IR (thin film): ν [cm⁻¹] 1055 (vs, ν_{BF}), 1106 (s, ν_{SO}), 1251 (w), 1404 (w), 1472 (m), 1608 (m), 1991 (vs, ν_{CO}), 2928 (m), 2987 (m), 3089 (w).

[Rh(S(O)NN*)(CO)] (8). [Rh(S(O)NN)(CO)][PF₆] (46 mg, 0.078 mmol) was dissolved in 5 mL of THF, and a solution of KOtBu (8.7 mg, 0.078 mmol) in 5 mL of THF was added at room temperature. The color changed immediately from yellow to deep red. The reaction mixture was stirred for 2 h, and all volatiles were removed *in vacuo*. The product was extracted with 15 mL of benzene, and all volatiles were removed *in vacuo* to yield 29 mg (90.1%) of a deep red powder. Crystals suitable for X-ray diffraction were grown from a saturated solution of **8** in toluene/pentane (1:1) at -30 °C. Anal. Calcd (%) for C₁₆H₂₅N₂SO₂Rh (412.36): C 46.60, H 6.11, N 6.79. Found: C 46.46, H 6.08, N 6.72. ¹H NMR (toluene-*d*₈, 500 MHz, 25 °C): δ 0.99 (t, 3 H, ³J_{HH} = 7.0 Hz, CH₂CH₃), 1.03 (t, 3 H, ³J_{HH} = 7.1 Hz, CH₂CH₃), 1.47 (s, 9 H, C(CH₃)₃), 2.07 (m, 1 H, CH₂CH₃), 2.29 (m, 3 H, CH₂CH₃), 2.87 (d, 1 H, ²J_{HH} = 14.9 Hz, CH₂N), 2.97 (d, 1 H, ²J_{HH} = 14.9 Hz, CH₂N), 4.13 (s, 1 H, CHS), 5.27 (d, 1 H, ³J_{HH} = 6.7 Hz, aryl-H₃), 5.96 (d, 1 H, ³J_{HH} = 8.8 Hz, aryl-H₅), 6.46 (m, 1 H, aryl-H₄). ¹³C{¹H} NMR (toluene-*d*₈, 126 MHz, 25 °C): δ 12.10 (CH₂CH₃), 12.40 (CH₂CH₃), 23.91 (C(CH₃)₃), 54.84 (CH₂CH₃), 55.84 (CH₂CH₃), 64.41 (CH₂N), 79.12 (d, ²J_{RhC} = 3.5 Hz, CHS), 98.66 (aryl-C₃), 110.06 (aryl-C₅), 134.56 (aryl-C₄), 156.48 (aryl-C₆), 163.30 (d, ⁴J_{RhC} = 1.6 Hz, aryl-C₂), 192.24 (d, ¹J_{RhC} = 72.6 Hz, CO). ESI-MS (*m/z*): 413.62 (100) [M]⁺, 357.49 (76) [M - C₄H₈]⁺. IR (thin film): ν [cm⁻¹] 996 (m), 1055 (s, ν_{SO}), 1174 (m), 1285 (w), 1379 (m), 1463 (s), 1532 (m), 1609 (m), 1974 (vs, ν_{CO}), 2860 (w), 2919 (m), 2963 (m).

X-ray Structural Analysis of X. Crystal Data. C₁₆H₂₅N₂O₂RhS, orange prisms, 0.2 × 0.1 × 0.1 mm³, triclinic, *P* $\bar{1}$, $a = 10.2627(1) \text{ Å}$, $b = 10.8734(2) \text{ Å}$, $c = 15.8663(3) \text{ Å}$, $\alpha = 89.5308(8)^\circ$, $\beta = 85.4696(10)^\circ$, $\gamma = 88.7646(19)^\circ$, from 8704 reflections, $T = 120(2) \text{ K}$, $V = 1764.55(5) \text{ Å}^3$, $Z = 4$, $fw = 412.35$, $D_c = 1.552 \text{ Mg/m}^3$, $\mu = 1.094 \text{ mm}^{-1}$.

Data Collection and Processing. Nonius KappaCCD diffractometer, Mo K α ($\lambda = 0.71073 \text{ Å}$), graphite monochromator, $-14 \leq h \leq 13$, $-14 \leq k \leq 14$, $-20 \leq l \leq 21$, frame scan width

= 1.0°, scan speed 1.0° per 60 s, typical peak mosaicity 0.51°, 40 767 reflections collected, 9353 independent reflections ($R_{\text{int}} = 0.058$). The data were processed with Denzo-Scalepack.

Solution and Refinement. Structure solved by Patterson method with SHELXS-97. Full matrix least-squares refinement based on F^2 with SHELXL-97; 415 parameters with no restraints, final $R_1 = 0.0390$ (based on F^2) for data with $I > 2\sigma(I)$ and, $R_1 = 0.0605$ on 9340 reflections, goodness-of-fit on $F^2 = 1.027$, largest electron density peak = $1.462 \text{ e } \text{Å}^{-3}$.

[Ir(S(O)NN*)(CO)] (9). A solution of KOtBu (14.7 mg, 0.131 mmol) in 4 mL of THF was added to a stirred suspension of [Ir(S(O)NN)(CO)][BF₄] (77.0 mg, 0.131 mmol) in 2 mL of THF. The color changed immediately to deep red, and the reaction mixture was stirred for 2 h at room temperature. Insoluble material was removed by filtration through cotton/Celite, and all volatiles of the filtrate were removed *in vacuo* to yield 54 mg (82.0%) of a deep red powder. Crystals suitable for X-ray diffraction were grown from a saturated solution of **9** in toluene/pentane (1:1) at -30 °C. ¹H NMR (toluene-*d*₈, 500 MHz, 25 °C): δ 0.99 (t, 6 H, ³J_{HH} = 7.1 Hz, CH₂CH₃), 1.50 (s, 9 H, C(CH₃)₃), 2.44 (m, 2 H, CH₂CH₃), 2.61 (m, 2 H, CH₂CH₃), 3.16 (d, 1 H, ²J_{HH} = 14.9 Hz, CH₂N), 3.26 (d, 1 H, ²J_{HH} = 14.9 Hz, CH₂N), 4.39 (s, 1 H, CHS), 5.32 (d, 1 H, ³J_{HH} = 6.6 Hz, aryl-H₃), 6.00 (d, 1 H, ³J_{HH} = 8.9 Hz, aryl-H₅), 6.42 (m, 1 H, aryl-H₄). ¹³C{¹H} NMR (toluene-*d*₈, 126 MHz, 25 °C): δ 12.03 (CH₂ CH₃), 12.35 (CH₂ CH₃), 24.19 (C(CH₃)₃), 56.68 (CH₂CH₃), 57.87 (CH₂CH₃), 63.16 (C(CH₃)₃), 66.27 (CH₂N), 81.32 (CHS), 98.63 (aryl-C₃), 110.65 (aryl-C₅), 134.68 (aryl-C₄), 156.90 (aryl-C₆), 164.41 (aryl-C₂), 185.64 (C=O). ESI-MS (*m/z*): 503.70 (70) [M]⁺, 447.58 (100) [M - C₄H₈]⁺. IR (thin film): ν [cm⁻¹] 834 (m), 1021 (m), 1063 (s, ν_{SO}), 1294 (w), 1378 (w), 1447 (m), 1480 (s), 1532 (m), 1608 (m), 1958 (vs, ν_{CO}), 2868 (w), 2928 (m), 2970 (m), 3064 (w).

X-ray Structural Analysis of 9. Crystal Data. C₁₆H₂₅N₂O₂IrS, orange prisms, 0.15 × 0.09 × 0.06 mm³, triclinic, *P* $\bar{1}$, $a = 10.2477(2) \text{ Å}$, $b = 10.8900(2) \text{ Å}$, $c = 15.8653(3) \text{ Å}$, $\alpha = 89.3335(11)^\circ$, $\beta = 85.4925(9)^\circ$, $\gamma = 88.7271(12)^\circ$, from 54 470 reflections, $T = 120(2) \text{ K}$, $V = 1764.55(6) \text{ Å}^3$, $Z = 4$, $fw = 501.64$, $D_c = 1.888 \text{ Mg/m}^3$, $\mu = 7.693 \text{ mm}^{-1}$.

Data Collection and Processing. Nonius KappaCCD diffractometer, Mo K α ($\lambda = 0.71073 \text{ Å}$), graphite monochromator, $-13 \leq h \leq 13$, $-14 \leq k \leq 14$, $-20 \leq l \leq 20$, frame scan width = 1.0°, scan speed 1.0° per 60 s, typical peak mosaicity 0.56°, 40291 reflections collected, 10 142 independent reflections ($R_{\text{int}} = 0.068$). The data were processed with Denzo-Scalepack.

Solution and Refinement. Structure solved by Patterson method with SHELXS-97. Full matrix least-squares refinement based on F^2 with SHELXL-97; 407 parameters with no restraints, final $R_1 = 0.0398$ (based on F^2) for data with $I > 2\sigma(I)$ and $R_1 = 0.0577$ on 8095 reflections, goodness-of-fit on $F^2 = 1.000$, largest electron density peak = $2.583 \text{ e } \text{Å}^{-3}$ and hole = $-2.821 \text{ e } \text{Å}^{-3}$.

[Rh(S(O)NN-d₂)(CO)][OAc-d₃] (10). **8** (20 mg, 0.049 mmol) was dissolved in acetic acid-*d*₄, resulting in an orange solution. According to the NMR spectrum of the reaction mixture, **8** was quantitatively converted to **10**. ¹H NMR (acetic acid-*d*₄, 500 MHz, 25 °C): δ 1.51 (s, 9 H, C(CH₃)₃), 1.60 (m, 6 H, CH₂CH₃), 3.14 (m, 3 H, CH₂CH₃), 3.37 (m, 1 H, CH₂CH₃), 4.37 (d, 1 H, ²J_{HH} = 17.0 Hz, CH₂N), 4.72 (d, 1 H, ²J_{HH} = 17.0 Hz, CH₂N), 7.66 (d, 1 H, ³J_{HH} = 8.3 Hz, aryl-H₅), 7.70 (d, 1 H, ³J_{HH} = 7.3 Hz, aryl-H₃), 8.15 (t, 1 H, ³J_{HH} = 7.8 Hz, aryl-H₄). ²D-NMR (acetic acid-*d*₄, 61 MHz, 25 °C): δ 5.16 (s, br, 1 D, CD₂S), 5.66 (s, br, 1 D, CD₂S). ¹³C{¹H} NMR (acetic acid-*d*₄, 126 MHz, 25 °C): δ 13.05 (CH₂ CH₃), 14.24 (CH₂ CH₃), 23.39

(C(CH₃)₃), 57.72 (CH₂CH₃), 58.35 (CH₂CH₃), 65.65 (quintd, ¹J_{DC} = 19.0 Hz, ²J_{RhC} = 4.0 Hz, CD₂S), 66.11 (d, ²J_{RhC} = 2.4 Hz, C(CH₃)₃), 66.60 (CH₂N), 121.87 (aryl-C₅), 122.66 (aryl-C₃), 143.24 (aryl-C₄), 156.23 (aryl-C₆), 162.84 (aryl-C₂), 188.79 (d, ¹J_{RhC} = 73.3 Hz, C=O). ESI-MS (*m/z*): 413.68 (100) [Rh(S(O)NN-*d*₁)(CO)]⁺ (due to measurement in a MeOH/acetic acid-*d*₄ mixture, one benzylic deuterium was exchanged by H), 62.30 (100) [AcO-*d*₃]⁻. IR (thin film): ν [cm⁻¹] 1038 (w), 1106 (s, ν_{SO}), 1166 (w), 1285 (w), 1387 (m), 1430 (m), 1472 (m), 1566 (s), 1702 (m), 2009 (vs, ν_{CO}), 2868 (w), 2936 (m), 2962 (m).

Acknowledgment. This work was supported by the DIP program for German-Israeli Cooperation, by the Donors of

the American Chemical Society Petroleum Research Fund, and by the Minerva Foundation. T.S. gratefully acknowledges the Minerva Foundation (Munich) for a Feodor-Lynen-Postdoctoral Fellowship. D.M. is the holder of the Israel Matz Professorial Chair of Organic Chemistry.

Supporting Information Available: (a) CIF files containing X-ray crystallographic data for compounds **4**, **6**, **8**, and **9**; (b) XYZ coordinates of all the computed complexes. This material is available free of charge via the Internet at <http://pubs.acs.org>.

OM701276S